

# Photoelectric conversion from a nitrobenzene dye monolayer modified ITO electrode

Deng-Guo Wu, Yan-Yi Huang, Chun-Hui Huang\* and Liang-Bing Gan

State Key Laboratory of Rare Earth Materials Chemistry and Applications, Peking University, Beijing 100871, China

An amphiphilic nitrobenzene dye ( $C_{18}H_{37}$ )<sub>2</sub>N—C<sub>6</sub>H<sub>4</sub>—CH=N—NH—C<sub>6</sub>H<sub>4</sub>—NO<sub>2</sub> has been synthesized and deposited on semiconducting transparent indium–tin oxide (ITO) electrodes by a Langmuir–Blodgett (LB) technique. Photocurrent generation was studied in a conventional photoelectrochemical cell. An action spectrum of the photocurrent generation is coincident with the absorption spectrum of the LB film-modified electrode, indicating that the dye aggregate in the LB film is responsible for the photocurrent. Some factors which may affect the observed photocurrent, such as the presence of O<sub>2</sub>, the concentration of methyl violet (MV<sup>2+</sup>), and hydroquinone (H<sub>2</sub>Q), pH and the bias voltage have been investigated. Models for the mechanism of photocurrent generation under different conditions are proposed.

It is known that some compounds not only show good performance in photoelectric conversion, but also show excellent behaviour in the field of non-linear optics. For example, squaraine, has been used practically in xerographic photo-receptors.<sup>1</sup> Recently, Ashwell has shown that this centrosymmetric molecule also has good second-order non-linear optical character.<sup>2</sup> Our group have systematically studied the photoelectric conversion properties of some dye molecules with second-order non-linear optical character and have found that the higher the molecular hyperpolarizability, the better the molecular photoelectric conversion efficiency.<sup>3–6</sup> The principle of second-harmonic non-linear optics indicates that the difference in the dipole moment of the molecule between the ground and excited states is one of the main factors for molecular hyperpolarizability.<sup>7,8</sup> On the other hand, photocurrent generation and charge dissociation are connected with the charge separation process,<sup>9,10</sup> which also requires a large dipole moment in the excited state. In order to obtain a better understanding of the relationship between molecular structure, second-order non-linear optical properties and the efficiency of photoelectric conversion, we have mainly studied hemicyanines, congeners and azopyridinium compounds with positive charge on the chromophore. As a part of our systematic study, we have now designed a dye molecule with electroneutral chromophores in which there is an electronic donor and an acceptor on each side of the molecule. This will provide experimental data for developing improved photoelectric conversion materials.

In this paper, we report an investigation of the photocurrent generation from an electroneutral dye LB film-modified ITO electrode. Mechanistic models for photocurrent generation under different conditions are proposed.

## Experimental

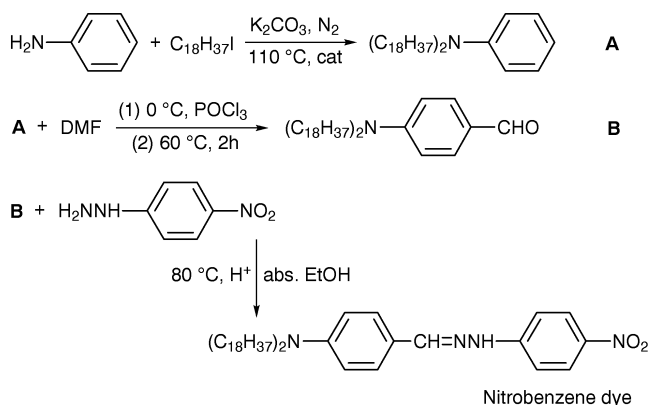
### Materials

( $C_{18}H_{37}$ )<sub>2</sub>N—C<sub>6</sub>H<sub>4</sub>—CH=N—NH—C<sub>6</sub>H<sub>4</sub>—NO<sub>2</sub> (dye 1) was synthesized by condensing *p*-nitrophenyl hydrazine with 4-(dioctadecaneamino)benzaldehyde in absolute ethanol. Hexadecyltrimethylammonium bromide was used as a phase transfer catalyst. The synthesis procedure is illustrated in Scheme 1. The product was purified by column chromatography on silica gel with dichloromethane as eluent. Elemental analysis: found: C, 77.41; H, 11.94; N, 7.12%. Calc. for C<sub>49</sub>H<sub>84</sub>N<sub>4</sub>O<sub>2</sub>: C, 77.31; H, 11.12; N, 7.36%. <sup>1</sup>H NMR

(CDCl<sub>3</sub>) δ: 0.86 (t, 6H, 2CH<sub>3</sub>), 1.21 (m, 60H, 30CH<sub>2</sub>), 1.57 (m, 4H, 2CH<sub>2</sub>), 3.30 (m, 4H, 2CH<sub>2</sub>N), 6.62 (d, 2H, phenyl-N), 7.05 (d, 2H, phenyl-N), 7.52 (d, 2H, phenyl-NO<sub>2</sub>), 7.71 (s, 1H, CH = N), 7.87 (b, 1H, NH), 8.15 (d, 2H, phenyl-NO<sub>2</sub>). Mp ca. 45–46 °C. The congeneric compound to dye 1 (CH<sub>3</sub>)<sub>2</sub>N—C<sub>6</sub>H<sub>4</sub>—CH=NNH—C<sub>6</sub>H<sub>4</sub>—NO<sub>2</sub> (dye 2) was synthesized by condensing *p*-nitrophenyl hydrazine with 4-(dimethylamino)benzaldehyde and purified as above. Mp ca. 179–180 °C. The identity of the product was confirmed by <sup>1</sup>H NMR and elemental analysis. The spreading solvent was chloroform. Distilled water was deionized water purified with an EASypure RF compact ultrapure system (*R* ≈ 18 MΩ). The electrolyte for the electrochemical experiment was KCl (AR). Hydroquinone (H<sub>2</sub>Q) (AR) was recrystallized from water before use. Methyl viologen diiodide (MV<sup>2+</sup>) was synthesized by the reaction of 4,4'-dipyridyl with excess methyl iodide in refluxing ethanol for 6 h. The product was filtered and washed with ethanol at least four times and its identity was confirmed by <sup>1</sup>H NMR analysis.

### Apparatus

C, H and N analysis of nitrobenzene dyes was carried out with a Carlo Erba 1106 elemental analyser. <sup>1</sup>H NMR spectroscopy was carried out using a Bruker ARX 400 BBI spectrometer. The electronic spectra were measured with a Shimadzu model 3100 UV–VIS–NIR recording spectrophotometer. The LB film-modified ITO electrode was fabricated by using a model 622 NIMA Langmuir–Blodgett trough. The light source used for the photoelectrochemical study was a



Scheme 1 Synthesis of nitrobenzene dye

500 W Xe arc lamp, the light beam was passed through a group of monochromatic filters (*ca.* 300–800 nm, Toshiba Co., Japan, and Schott Co., USA) in order to get a given bandpass of light. The light intensity at each wavelength was calibrated with an energy and power meter (Sciencetech, USA).

### LB film preparation

A solution of dye 1 (0.712 mg ml<sup>-1</sup> in chloroform) was spread dropwise onto the clean water subphase by syringe at a subphase temperature of *ca.* 20 °C. The chloroform was allowed to evaporate for 15 min and the monolayer was then compressed. The substrates for monolayer deposition were transparent electrodes of ITO-coated borosilicate glass and the sheet resistance was 50 Ω cm<sup>-2</sup>. The ITO plates were cleaned using detergent and chloroform, followed by rinsing with pure water. To ensure the formation of a hydrophilic surface, the plates were immersed for 2 days in a saturated sodium methanol solution and then thoroughly ultrasonicated with pure water several times.

For deposition of the monolayer, the ITO slide was first immersed in the subphase; a single monolayer was formed and compressed to 23 mN m<sup>-1</sup>. The slide was then raised at a rate of 4 mm min<sup>-1</sup>. Only films having transfer ratios of 1.0 ± 0.1 were used in the experiments.

### Photoelectrochemical and electrochemical measurements

A conventional glass three-electrode cell (30 ml capacity) having a flat window for illumination of the working electrode was used. The electrical connection to the ITO working electrode was obtained by mechanical contact with a clip, the illuminated area was 0.38 cm<sup>2</sup>. The counter-electrode was a polished Pt wire and the reference was a saturated calomel electrode (SCE). All photoelectrochemical data were recorded using a model CH 600 voltammetric analyser controlled by computer. Cyclic voltammetry (CV) experiments were performed on an EG&GPAR 273 potentiostat/galvanostat with EG&GPAR 270 electrochemical software. The supporting electrolyte was an aqueous solution of 0.5 M KCl. Unless specified, oxygen was removed from the solutions by bubbling N<sub>2</sub> before every measurement.

## Results and Discussion

### Characterization of LB film and dye-ITO electrode

Surface pressure measurements on monolayers were used to determine the average values of the area per molecule occupied by the dye at the air/water interface. Fig. 1 shows a typical surface pressure–area ( $\pi$ - $A$ ) isotherm for dye 1. The limiting area per molecule is 45 Å<sup>2</sup>, which agrees with that for

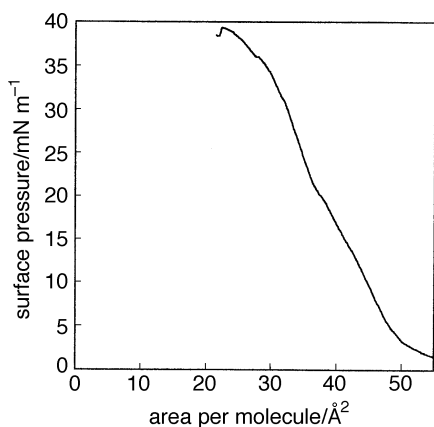


Fig. 1 Surface pressure–area isotherm of (C<sub>18</sub>H<sub>37</sub>)<sub>2</sub>N–C<sub>6</sub>H<sub>4</sub>–CH=N–NH–C<sub>6</sub>H<sub>4</sub>–NO<sub>2</sub> at the air/water interface (20 ± 1 °C)

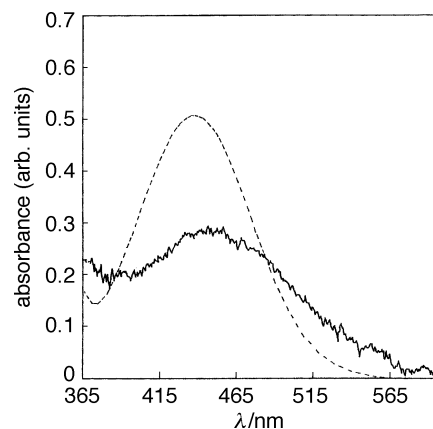


Fig. 2 Absorption spectroscopy of (C<sub>18</sub>H<sub>37</sub>)<sub>2</sub>N–C<sub>6</sub>H<sub>4</sub>–CH=N–NH–C<sub>6</sub>H<sub>4</sub>–NO<sub>2</sub> on ITO substrate (—) and in chloroform solution (...)

a similar compound (C<sub>16</sub>H<sub>33</sub>)<sub>2</sub>N–C<sub>6</sub>H<sub>4</sub>–CH=CH–C<sub>5</sub>H<sub>4</sub>N–(CH<sub>2</sub>)<sub>2</sub>–COO<sup>-</sup> reported by Bubeck *et al.*,<sup>11</sup> It can be clearly seen that there is a plateau in the  $\pi$ - $A$  curve, indicating that the dye molecules reorientate on the water surface above 20 mN m<sup>-1</sup> surface pressure, since the nitrobenzene molecule has two hydrophilic radicals (–NO<sub>2</sub> and –NH).

The  $\lambda_{\max}$  of the LB film in a UV–VIS absorption spectrum is at 450 nm while the  $\lambda_{\max}$  of the dye in chloroform is at 430 nm (Fig. 2), indicating the presence of J-aggregates.<sup>12</sup>

### Electrochemical properties of the dye

In order to estimate the redox potentials of the excited-state dye and to discuss the mechanism of photocurrent generation, CV studies were carried out. Typical voltammograms are shown in Fig. 3. Monolayer dye-ITO was used as a working electrode in 0.5 M KCl aqueous solution. The pH of the electrolyte solution was adjusted to pH *ca.* 2 with dilute HCl solution in the acidic system. The redox potentials of the couples dye/dye<sup>-</sup> and dye/dye<sup>+</sup> are –0.35 and 0.80 V *vs.* SCE, respectively, in a neutral medium. It can be seen from Fig. 3 that the CV curve was shifted towards positive voltage in an acidic medium compared with that in a neutral medium. The reduction peak was shifted by *ca.* 136 mV while the oxidation peak was only shifted by *ca.* 32 mV. The positive shift of the reduction peak indicates that a proton is involved in the redox reaction and the reduction reaction takes place more easily in an acidic rather than a neutral medium.<sup>13</sup>

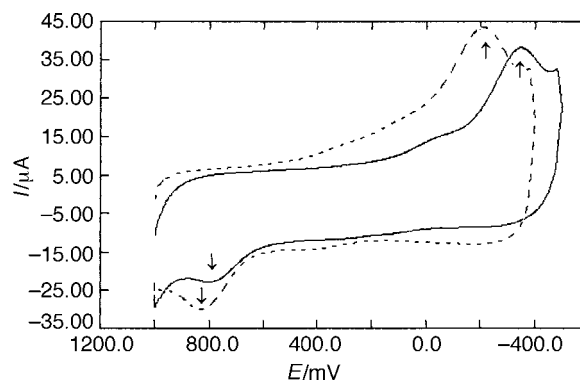


Fig. 3 CV of the dye 1 monolayer on ITO substrate as working electrode in 0.5 M KCl aqueous solution. (—) Neutral solution and (...) pH *ca.* 2 solution. Sweep rate = 100 mV s<sup>-1</sup> (↑ reduction peak, ↓ oxidation peak).

### Photocurrent generation from dye-ITO electrode

A steady cathodic photocurrent ranging from 89 to 160 nA cm<sup>-2</sup> was obtained from the dye monolayer-modified electrode when the dye-ITO electrode was illuminated, by white light under 110 mW cm<sup>-2</sup> light intensity and without any bias voltage, in 0.5 M KCl electrolyte solution. The photoelectric response was very stable when switching on and off many times, as shown in Fig. 4. Fig. 5 shows the action spectrum of the cathodic photocurrents. The spectrum responses coincide with the absorption spectrum (Fig. 2) suggesting that the aggregate of the dye in the LB film is responsible for photocurrent generation. A photocurrent of ca. 49.7 nA cm<sup>-2</sup> can be obtained under  $1.14 \times 10^{16}$  photons cm<sup>-2</sup> s<sup>-1</sup> irradiation at 464 nm by white light of 110 mW cm<sup>-2</sup> intensity, through a band-pass filter (KL45 + GG420) in 0.5 M KCl electrolyte solution with zero bias voltage. The attainment of such a photocurrent means that the quantum yield, which is cited per absorbed photon, is ca. 0.24% for the monolayer dye-modified electrode (the absorbance ratio of the film is ca. 1.13% for the incident light at 464 nm).

### Effect of bias voltage

In order to determine the polarity of the current flow, the effect of bias voltage was investigated. A plot of photocurrent vs. electrode potential is shown in Fig. 6. The photocurrent is cathodic in the range from -100 to ca. +30 mV. The anodic current can be observed and it increases with increasing positive bias voltage. When -100 mV bias voltage was applied to the electrode, ca. 62.1 nA cm<sup>-2</sup> photocurrent was obtained at 464 nm. In this case the quantum yield reaches ca. 0.30%. This

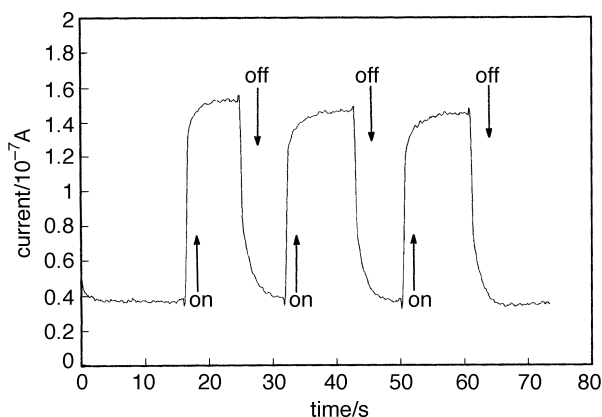


Fig. 4 Photocurrent generation from the dye 1 LB-ITO electrode upon irradiation with white light at 110 mW cm<sup>-2</sup> (↑ light switching on and ↓ light switching off)

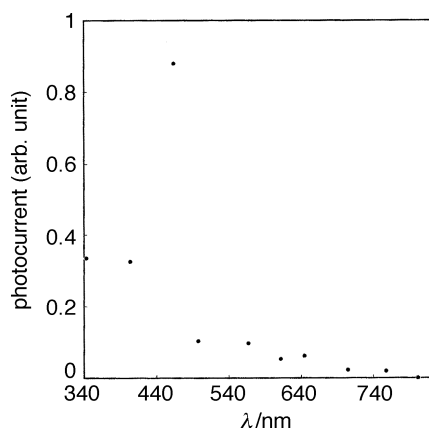


Fig. 5 Action spectrum of the cathodic photocurrents. (The photocurrents and the intensities of different wavelength are all normalized.)

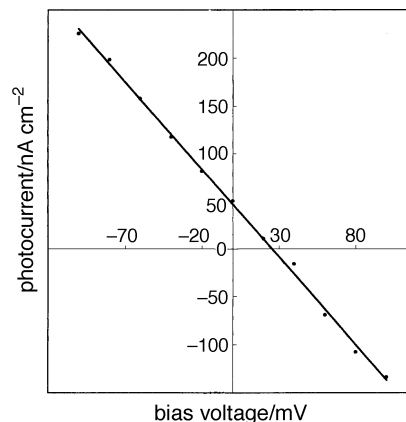


Fig. 6 Photocurrent vs. electrode potential for LB film of dye 1 on ITO

may result from the applied negative voltage which is in the same direction and can accelerate the electronic flow, forming a strong electric field in the space charge region within the LB film. Such a strong electric field may accelerate the photoinduced charge separation and decrease the probability of charge recombination before the target electron acceptors are reached.

### Effect of electron donors and acceptors

Fig. 7 shows the dependence of the photocurrent on MV<sup>2+</sup> concentration. It is seen that the photocurrent increases with increasing MV<sup>2+</sup> concentration. For comparison with the effect of oxygen on the photocurrent, the photocurrent was measured both under ambient conditions and in the absence of the oxygen (N<sub>2</sub> gas was used to remove O<sub>2</sub> from the electrolyte solution). The results indicate that the quantum yield for effective electron injection is higher in the presence of oxygen because it acts as an electron acceptor through the formation of a superoxide anion radical.<sup>14</sup> If the electrolyte solution was saturated with oxygen, by bubbling oxygen, the photocurrent was noticeably increased by ca. 50%, indicating that O<sub>2</sub> is a favourable factor in the electron transfer process.

When H<sub>2</sub>Q was added to the electrolyte solution the photocurrent tended to decrease under ambient conditions and quickly decreased and became an anodic current in the absence of oxygen. Fig. 8 shows the dependence of the photocurrent on the H<sub>2</sub>Q concentration. In order to further confirm this observation, the effect of the electron-donor K<sub>4</sub>[Fe(CN)<sub>6</sub>] on the photocurrent of the LB film was measured; the photocurrent quickly decreased with increasing K<sub>4</sub>[Fe(CN)<sub>6</sub>] concentration and even became an anodic current under ambient

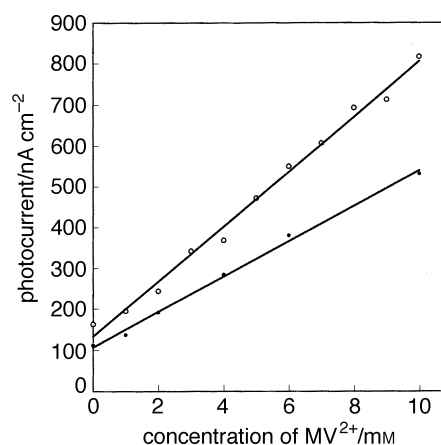
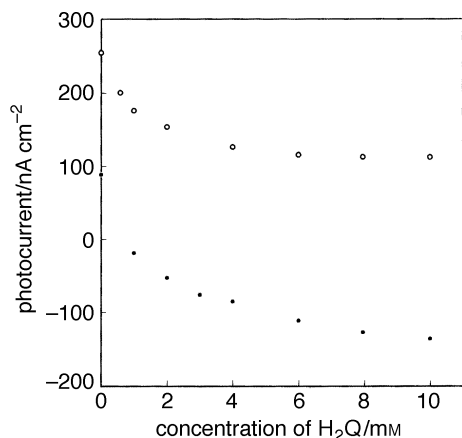


Fig. 7 Relationship between MV<sup>2+</sup> concentration and photocurrent. (○) Under ambient conditions, (●) in the absence of oxygen.



**Fig. 8** Dependence of the photocurrent on the H<sub>2</sub>Q concentration. (○) Under ambient conditions, (●) in the absence of oxygen.

conditions, indicating that the presence of an electron donor is unfavourable to the production of a cathodic photocurrent in the system.

### Effect of pH

The effect of pH on the photocurrent of the monolayer was investigated in a Britton–Robinson buffer solution containing 0.5 M KCl. It is seen, in Fig. 9, that the photocurrent decreases quickly with increasing pH. At pH *ca.* 4, anodic and cathodic spikes were observed on commencement and interruption of illumination, respectively. The current changes sign and becomes anodic at pH *ca.* 5. This indicates that an acidic medium is favourable to the production of a cathodic current while a weak acidic or alkaline medium is not. Under favourable conditions, *e.g.* pH *ca.* 2, in the presence of O<sub>2</sub> and 5 mmol l<sup>-1</sup> MV<sup>2+</sup>, with a -100 mV bias voltage, then a photocurrent of *ca.* 121 nA cm<sup>-2</sup> was obtained under 464 nm irradiation; the quantum yield was 0.58%. Note that dissolved oxygen has little effect on the photocurrent in the acidic system. This may be because the oxygen molecule combines with H<sup>+</sup> ion to form HO<sub>2</sub><sup>+</sup> ion, decreasing the electron-accepting ability of the oxygen. Since an alkaline medium has no effect on the electron-accepting ability of oxygen, the effect of dissolved oxygen on the photocurrent was observed in an alkaline system.

### Effect of the media on the UV–VIS spectrum

Since dye 1 is insoluble in polar solvent, a congener of dye 1 was used for the following experiments. In order to discuss the effect of the solvent on photocurrent generation, the UV–VIS spectra of dye 2 were measured in different solvents. The main absorption band is increasingly red-shifted with increasing polarity of the solvent. For example, the peak is at 421.4 nm

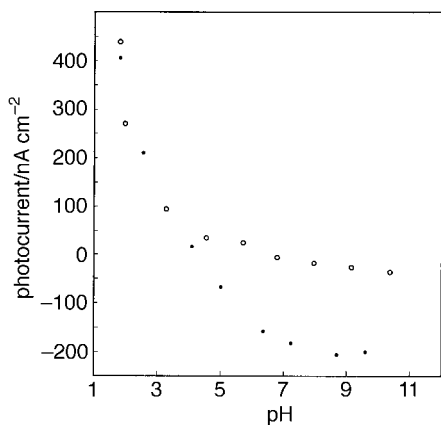


**Fig. 9** Effect of pH on the photocurrent in Britton–Robinson buffer solution: (○) under ambient conditions, (●) in the absence of oxygen

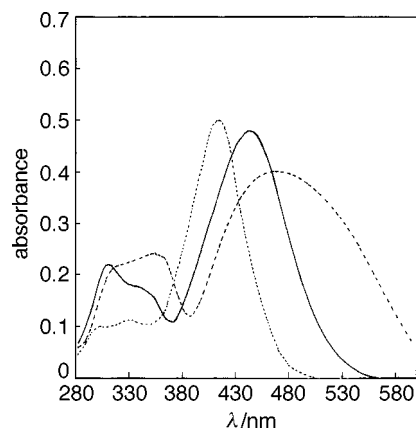
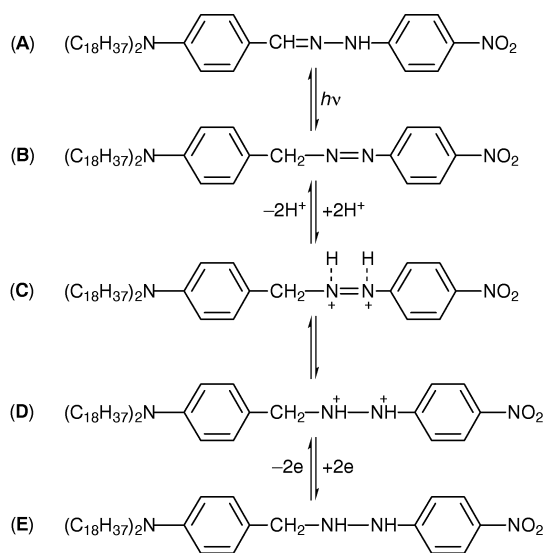


**Fig. 10** Effect of the media on UV–VIS spectrum, (—) ethanol solution, (...) pH *ca.* 2 solution, (---) pH *ca.* 10 solution

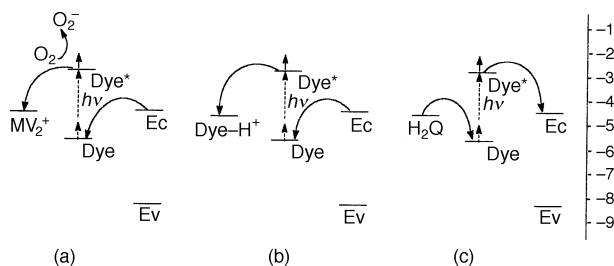
in benzene, 430.0 nm in chloroform and 442.9 nm in ethanol. The weaker absorption band has a tendency to be blue-shifted with increasing polarity of the solvent, indicating that the main absorption band corresponds to a  $\pi \rightarrow \pi^*$  transition and the weaker one to an  $n \rightarrow \pi^*$  transition.<sup>15</sup> Furthermore, the  $\pi \rightarrow \pi^*$  transition absorption band shows a blue-shift ( $\Delta\nu = 28.6$  nm) in an acidic medium (pH *ca.* 2), a red-shift ( $\Delta\nu = 35.7$  nm) and becoming broad in an alkaline medium (pH *ca.* 10), compared with that in ethanol solution. The relative height of the  $n \rightarrow \pi^*$  to  $\pi \rightarrow \pi^*$  transition band is less in an acidic medium than in an alkaline medium (Fig. 10). This indicates that the conjugation of dye 2, compared with a neutral medium (ethanol solution), is decreased in an acidic medium and increased in an alkaline medium. No detectable spectral change in ethanol solution was observed after 1 h of irradiation at 464 nm, indicating that the conjugation effect of dye 2 is unchanged on irradiation.

### Mechanism of photocurrent generation from the dye–ITO electrode

Since there is no detectable spectral change after irradiation of the dye solution, it is concluded that there is no *trans* → *cis* photoisomerization occurring. A photoinduced tautomerism, as shown in Scheme 2, may take place. Upon irradiation **A** absorbs energy from the excitation light and undergoes tautomerism involving an intramolecular shift of a hydrogen atom between alternative binding sites to form **B**. In an acidic medium, **B** may accept protons to become **C**, which is an elec-



**Scheme 2**



**Scheme 3** Schematic diagram showing electron transfer processes. Arrows indicate the electron flow. (a) and (b) cathodic photocurrent, (Dye-H<sup>+</sup>) represents the state of dye 1 which combines with H<sup>+</sup> ions in acidic medium, (c) anodic photocurrent.

tron acceptor and thus assists generation of a cathodic photocurrent. This mechanism is also supported by the spectrum change in an acidic medium. **C** and **D** have a resonance structure which accepts electrons to become **E**.

The direction of the photocurrent generation is shown in Scheme 3. We can see that it depends not only on the dye sensitized by light, but also on the nature of the redox couple in the aqueous phase surrounding the electrode. In the presence of redox couples favouring electron donation an anodic photocurrent is generated, while with electron acceptors in the aqueous phase a cathodic photocurrent is produced.

In order to examine the mechanism of light sensitization for the production of cathodic and anodic photocurrents, the energies of the relevant electronic states must be estimated. From the electron affinity the conduction band ( $E_c$ ) and valence band ( $E_v$ ) edges of the ITO electrode surface are estimated to be *ca.*  $-4.5$  and  $-8.3$  eV,<sup>16</sup> respectively. The energy levels of the dye are assumed to be  $-5.54$  eV ( $0.80$  V *vs.* SCE) and  $-2.78$  eV on the absolute scale, respectively, with reference to an oxidation potential of  $0.80$  V *vs.* SCE and a band gap of  $2.76$  eV ( $450$  nm). The reduction potential of the dye in an acidic medium is  $-4.52$  eV ( $-0.22$  V *vs.* SCE), the reduction potential of  $MV^{2+}$  is  $-4.51$  eV ( $-0.23$  V *vs.* SCE),<sup>17</sup> the oxidation potential of  $H_2Q$  is  $-4.61$  eV ( $-0.13$  V *vs.* SCE)<sup>17</sup> on the absolute scale.

The cathodic photocurrent probably involves electron transfer from the excited dye aggregate to the electron acceptor, with a subsequent electron transfer from the conduction band of the ITO electrode to the hole residing in the dye aggregate<sup>17</sup> in the presence of some electron acceptors, such as  $O_2$ ,  $MV^{2+}$  and in an acidic medium.

Anodic photocurrent generation may occur when an electron donor injects an electron into the hole of the ground-state dye aggregate with subsequent electron transfer from the excited dye aggregate to the conduction band of the ITO electrode,<sup>17</sup> in the presence of some electron donors, such as  $H_2Q$ ,  $K_4[Fe(CN)_6]$  and in an alkaline medium.

## Conclusions

The results suggest that the mechanism of generation of a cathodic photocurrent from the dye-ITO electrode involves the formation of excited-state tautomerism. This state accepts an electron from the conductive band of the ITO electrode and, meanwhile, transfers an electron to the electrolyte solution through the LB film. The mechanism is supported by studying the effect of bias voltage, the addition of donors and acceptors, and pH, on the photocurrent generation. The quantum yield is  $0.58\%$  under favourable conditions.

This project is financially supported by a National Fundamental Research Key Project of China and the National Natural Science Foundation of China (No. 29671001)

## References

- 1 K. Y. Law, *Chem. Rev.*, 1993, **93**, 449.
- 2 G. J. Ashwell, G. Jefferies, D. G. Hamilton, D. E. Lynch, M. P. S. Roberts, G. S. Bahra and C. R. Brown, *Nature (London)*, 1995, **375**, 385.
- 3 W. S. Xia, C. H. Huang, L. B. Gan and H. Li, *J. Chem. Soc., Faraday Trans.*, 1996, **92**, 3131.
- 4 W. S. Xia, C. H. Huang and D. J. Zhou, *Langmuir*, 1997, **13**, 80.
- 5 W. S. Xia, C. H. Huang, X. Z. Ye, C. P. Luo, L. B. Gan and Z. F. Liu, *J. Phys. Chem.*, 1996, **100**, 2244.
- 6 W. S. Xia, C. H. Huang, L. B. Gan, H. Li and X. S. Zhao, *J. Chem. Soc., Faraday Trans.*, 1996, **92**, 769.
- 7 *Organic Materials for Nonlinear Optics III* ed. G. J. Ashwell and D. Bloor, Royal Society of Chemistry, Cambridge, 1993.
- 8 P. N. Prasad and D. J. Williams, *Introduction to Nonlinear Optical Effects in Molecules and Polymers*, Wiley, New York, 1991.
- 9 S. Nešpůrek, *Int. J. Electron.*, 1994, **76**, 777.
- 10 S. Allen, in *Molecular Electronics*, ed. G. J. Ashwell, Research Studies, Taunton, 1992, pp. 207–265.
- 11 C. Bubeck, A. Laschewsky, D. Lupo, D. Neher, P. Ottenbreit, W. Paulus, W. Prass, H. Ringsdorf and G. Wegner, *Adv. Mater.*, 1991, **3**, 54.
- 12 A. Haraguchi, Y. Yonezawa and R. Hanawa, *Photochem. Photobiol.*, 1990, **52**, 307.
- 13 Y. Li and S. Dong, *J. Electroanal. Chem.*, 1993, **348**, 181.
- 14 (a) H. Hada and Y. Yonezawa, *Synth. Met.*, 1987, **18**, 791; (b) H. Hada, Y. Yonezawa and H. Inaba, *Ber. Bunsen-Ges. Phys. Chem.*, 1981, **85**, 425.
- 15 (a) N. S. Bayliss and E. G. Mcrae, *J. Phys. Chem.*, 1954, **58**, 1002; (b) G. J. Brealey and M. Kasha, *J. Am. Chem. Soc.*, 1955, **77**, 4462.
- 16 L. Sereno, J. J. Silber, L. Otero, M. D. V. Bohorquez, A. L. Moore, T. A. Moore and D. Gust., *J. Phys. Chem.* 1996, **100**, 814.
- 17 Y. S. Kim, K. Liang, K. Y. Law and D. G. Whitten, *J. Phys. Chem.*, 1994, **98**, 984.

Paper 7/08450A; Received 24th November, 1997